JOURNAL OF AIRCRAFT
Vol. 48, No. 4, July–August 2011

Improved Range Equation Based on Aircraft Flight Data

William E. Randle,* Cesare A. Hall,† and Maria Vera-Morales‡
University of Cambridge, Cambridge, England CB2 1ST, United Kingdom

DOI: 10.2514/1.C031262

This paper uses measurements from flight-data recorders to develop an improved, simple model for aircraft fuel burn. The model is an adaptation of the Bréguet range equation, with straightforward adjustments made for headwind, cruise flight conditions, climb performance, and descent operation. The adjustments made are based on physical reasoning combined with results from real flight operations. The analysis of flight data shows that the additional fuel burn required for takeoff and climb is constantly around 1.5% of takeoff weight. The fuel burn during descent shows greater variation and there appears to be scope for improvements through more consistent approach procedures. The new model is validated against fuel-burn data from a large number of flights and is shown to have greatly improved accuracy relative to a simple form of the Bréguet range equation.

Nomenclature

A_w	=	aircraft wing area
C_L	=	aircraft lift coefficient
D	=	drag
g	=	acceleration due to gravity
H	=	range factor
h	=	altitude
k_{cl}	=	climb/cruise range parameter ratio
L	=	lift
M	=	Mach number
p	=	atmospheric pressure
R	=	air gas constant
s	=	distance
T	=	atmospheric temperature
V	=	velocity, flight speed
W	=	weight
γ	=	ratio of specific heats
Δ	=	incremental factor
ε	=	error
η	=	engine overall efficiency
σ	=	standard deviation

Subscripts

air	=	relative to the air
cl	=	climb
cr	=	cruise
d	=	descent
EOC	=	end-of-cruise
f	=	Final
gc	=	great circle
gr	=	relative to the ground
HW	=	headwind
i	=	initial, value recorded for event i
lost	=	lost (during climb)
nom	=	nominal
rec	=	recovered
TO	=	takeoff
TOC	=	top-of-climb

Received 5 October 2010; revision received 3 March 2011; accepted for publication 4 March 2011.

*Student, Department of Engineering, Whittle Laboratory.
†University Lecturer, Department of Engineering, Whittle Laboratory. Member AIAA.
‡Lecturer in Engineering, Aeronautical and Automotive Engineering Department, Loughborough University.

I. Introduction

THE conditions that represent the optimum trajectory for long-range, high-subsonic-speed flight have attracted much interest for many years. The first studies aimed at estimating aircraft cruise range took place between 1918 and 1922 [1]. In 1923 Bréguet published work on a proposed range equation [2], which later became known as the classical Bréguet range equation. This was further developed by authors Page [3] and Edwards [4] in the United Kingdom and Jonas [5] and Perkins and Hage [6] in the United States. The equations presented in these early studies relied on either a cruise-climb technique with constant Mach number and lift coefficient or a constant-altitude constraint with constant lift coefficient but continuously decreasing airspeed.

In 1974, Peckham [7] expanded on Edwards's [4] work and adapted the theory for the more common cruise regime of constant altitude and constant Mach number. Further modification of the range equation was made by Torenbeek [8] after a comprehensive analysis of the optimum cruise performance. Torenbeek used an analytical approach, combining the analysis of range performance based on cruise regime with an estimate of the fuel used during takeoff, climb and maneuvering. An energy balance was used to account for the so-called lost fuel used to transfer the aircraft to a cruising height and speed. Although Torenbeek presented a sophisticated remodeling of the range equation, his analysis neglected the effect of wind on the performance of the aircraft. Rivas et al. [9] addressed this problem through a detailed analysis of the effect of wind on the drag polar for each cruise regime. They concluded that the maximum range increases with tailwind and analogously decreases with headwind: an unsurprising outcome, yet significant due to the analytical technique used to derive the results.

Although the Bréguet range equation is very simple in its derivation and application, it is widely used to assess the performance of a proposed aircraft configuration (in terms of maximum range for a given payload) in the preliminary design stages. Martinez-Val et al. [10] recently used this equation to assess the variation of performance for different jet airliners, deriving an efficiency characteristic termed the *range factor*, elaborated from available manufacturer data. This was done by decomposing the maximum takeoff weight into several parameters (payload, fuel load, etc.), combined with some key points taken from the aircraft payload-range diagram. The range factor thus derived by Martinez-Val et al. captures the aerodynamic and propulsive efficiencies of the aircraft and enables, using the Bréguet range equation, the prediction of maximum range, or the prediction of fuel burn for a given range.

Other recent studies applying forms of the range equation include Cavcar and Cavcar [11], who compared different cruise range solutions for high-subsonic-Mach-number aircraft, and Poll [12], who used developments to the Bréguet range equation to assess the potential for aircraft total fuel-burn reduction through advances in technology, air traffic management, and fundamental changes to passenger aircraft design.

Although not specifically studying the range equation, Reynolds [13] conducted research into the inefficiency caused by nonoptimal flight trajectories. His work compared fuel burn from flight data with a theoretical minimum derived from aircraft performance models. He estimated the extra fuel needed for climb, cruise, and descent separately and introduced a fuel-based metric instead of the typically used flight-distance-based metric.

The key aim of the current paper is to produce an improved simple model that can be applied to any given flight and aircraft type to predict the fuel burn with a known level of accuracy. A large sample of flight-data recorder (FDR) measurements from various high-subsonic-speed turbofan aircraft has been made available. In this paper, analysis of this flight data together with physical reasoning are used to develop modifications to the classical Bréguet range equation. The result is a simple, yet robust, model that predicts the fuel burn for a complete flight, given a few known basic parameters. In addition, through the analysis of flight data the paper aims to identify where aircraft are not performing as expected and where there may be scope for fuel-burn reductions. As far as the authors are aware, there is no previous published work that uses measured flight data to assess and improve simple fuel-burn models, and therefore this paper makes a new contribution to the field of aircraft flight performance. It should be of interest to airlines, aircraft manufacturers, and academic researchers involved in performance modeling and analysis.

The paper starts with the classical range equation and derives a form of this that can be used for determining fuel burn. The problem of converting the flight data into an appropriate form for analysis is then considered: in particular, the method needed to isolate the various phases of a flight. The range factor, a key parameter in this report, is calculated from the flight data and compared with values determined from manufacturer's data [10]. Several adaptations to the range equation are then developed. The effects of wind, cruise conditions, lost fuel during takeoff and climb, and operational inefficiencies during descent are investigated. Finally, the new model is validated against a large alternative database of FDR data, and its accuracy is compared with the Bréguet range equation.

II. Bréguet Range Equation

The classical range equation is commonly presented in the following formula [10], where s is the range, V is the flight speed, sfc is the specific fuel consumption, L/D is the lift-to-drag ratio, and W_i and W_f are the weight of the aircraft at the initial and final stages of the cruise, respectively:

$$s = \int_{W_f}^{W_i} \frac{V(L/D)}{g\,\mathrm{sfc}} \frac{\mathrm{d}W}{W} \tag{1}$$

If the airspeed, lift-to-drag ratio, and specific fuel consumption remain constant during cruise, the equation can be integrated to give

$$s = H\,\ell_n\left(\frac{W_i}{W_f}\right) \tag{2}$$

where H is the range factor [10]. This represents the nominal aircraft performance during cruise and is equal to

$$H = \frac{V(L/D)}{g\,\mathrm{sfc}} = \frac{\eta(L/D)\mathrm{LCV}}{g} \tag{3}$$

This is a key parameter in this paper, as it will be used as the basis for the prediction of fuel-burn rate. It is an attractive property, as it can account for the mean propulsive and aerodynamic characteristics of the complete aircraft without any detailed information about drag polars, engine efficiencies, etc.

Given a known distance and range factor, the range equation can be used to predict fuel burn. Rearranging Eq. (2) leads to the following:

$$\frac{W_f}{W_i} = \exp\left\{\frac{-s}{H}\right\} \tag{4}$$

The weight of burned fuel, W_{fuel}, is defined as the difference between the initial and final weights of the aircraft:

$$W_{\mathrm{fuel}} = W_i - W_f \tag{5}$$

Equation (4) can be combined with Eq. (5) and rearranged further, giving the predicted fuel burn for a given distance:

$$W_{\mathrm{fuel}} = W_i\left(1 - \exp\left\{\frac{-s}{H}\right\}\right) \tag{6}$$

Note that the equation is only valid for the cruise phase, as it relies on the assumption of constant H. However, for long-haul flights, the cruise distance forms the large majority of the flight, and so the equation can give a good approximation of the fuel burn if the cruise distance s_{cr} is taken as the overall great-circle distance s_{gc} and if the initial weight of cruise W_i is taken as the weight at takeoff W_{TO}. Adjusting Eq. (6) to use the parameters described above gives the following equation that will be the basis of the fuel-burn model for this paper:

$$W_{\mathrm{fuel}} = W_{\mathrm{TO}}\left(1 - \exp\left\{\frac{-s_{\mathrm{gc}}}{H}\right\}\right) \tag{7}$$

Further adjustments will be made to this equation, building on the literature described above to present a model that is not only theoretically sound, but is also validated by the large amount of FDR data that have been made available.

III. Flight-Data Processing

The FDR data for this study were provided by Swiss International Air Lines, Ltd. Airbus and Boeing aircraft are included operating domestic and international routes ranging from a few hundred to thousands of kilometers. Table 1 shows the various aircraft models analyzed and the size of the flight samples.

The FDR data for each flight were given in matrix form with the columns representing the different flight parameters recorded and the rows corresponding to specific points in time (events) when the data were acquired. The flight parameters recorded ranged from engine temperatures and pressures to latitude, longitude, and airspeed. These parameters were recorded more frequently during phases with greater variation among the parameters. For example, during takeoff and climb, data were logged every 5 s, whereas during cruise, the sample intervals could be up to 40 s. There are more than 1000 data acquisition events in each flight.

Although the accuracy of many of the recorded flight parameters is unknown, the measurement of fuel flow should be correct to within 1% of cruise fuel flow (see [14]). It is also expected that parameters such as the aircraft latitude, longitude, and altitude should be accurate, given that these are derived from Global Positioning System and barometric altimeter data. Other parameters are of secondary importance to the fuel-burn analysis.

A. Identifying the Flight Phases

It is first necessary to identify the cruise phase for each flight. This phase is defined as the period between the top-of-climb and the start-of-descent. Defining the cruise in this way allows for a stepped

Table 1 Aircraft FDR data included in the study

Aircraft	Acronym	Number of flights
A320-214	A320	163
A330-243	A330	185
A340-300	A340	130
B757-200	B757	113
B767-300	B767	151
B777-300	B777	144

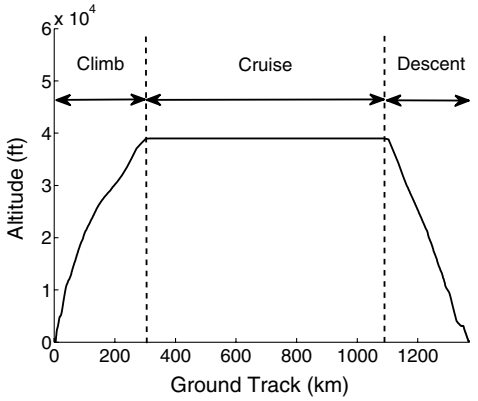

Fig. 1 Deconstruction of an A330 flight into three phases using the FDR data.

cruise, favored for many long-haul flights due to the greater efficiency it allows while remaining within air traffic control (ATC) constraints. The takeoff and climb phase is defined as the period between the start of the takeoff run and the top-of-climb, and the descent and approach are incorporated into the third final phase, encompassing the period from the top-of-descent to touchdown. This is shown graphically in Fig. 1.

The cruise phase was isolated using a MATLAB code to identify the two aforementioned points in the flight. This was done initially by searching for the first or last event after takeoff in which the absolute rate of climb or descent was below 10 ft/s for a given time period. This value was chosen by comparing plots of climb rate against ground-track distance for several different flights and aircraft types and then assessing the average climb rate after the aircraft had leveled out for cruise. Using 10 ft/s as a threshold climb/descent rate allowed for small perturbations in cruise altitude, due to external factors such as turbulence, while still ensuring that the aircraft would only have a vertical speed greater than this value if it was in a steady climb or descent.

The method was further refined to only start searching for the climb or descent-rate criteria when the aircraft was flying above 25,000 ft and above a Mach number of 0.65. These values were chosen because they fall just below the minimum average cruise altitude and the lowest average cruise speed for the range of aircraft considered. These additional criteria increased the robustness of the code and eliminated any misidentification of the cruise phase.

With the cruise phase identified, the relevant parameters were calculated for each flight. The Haversine formula [15] was used to calculate ground-track and great-circle distance using the latitude and longitude of the aircraft.

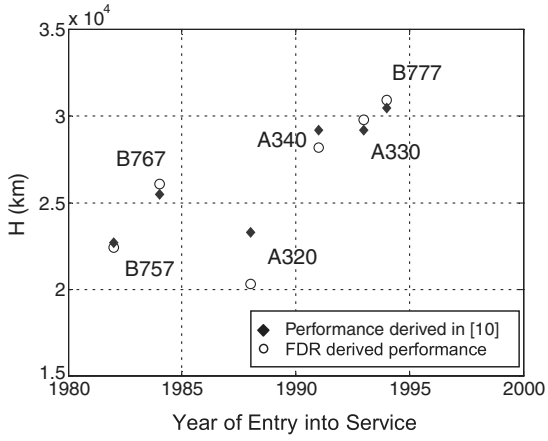

Fig. 2 Aircraft range factors calculated from manufacturer and FDR data.

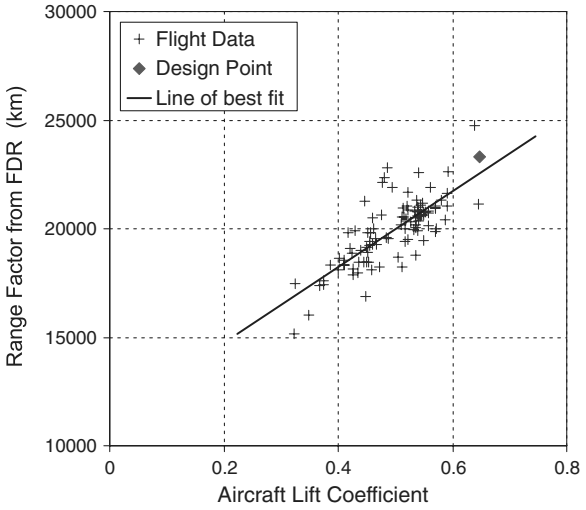

Fig. 3 Variation of range factor with cruise lift coefficient for the A320 flights.

B. Variation in Range Factor

The range factor H was calculated directly from flight data by rearranging Eq. (2) to give

$$H = \frac{s}{\ell_n(W_{\mathrm{TOC}}/W_{\mathrm{EOC}})} \tag{8}$$

where s in this case is the cruise ground-track distance for each flight, and W_{TOC} and W_{EOC} are the gross weights of the aircraft recorded at the start-of-cruise and end-of-cruise. H is a critical parameter and it is worthwhile to compare the mean values obtained from the flight data with those obtained from the aircraft payload-range diagrams [10], as shown in Fig. 2. For all aircraft types except the A320, there is a reasonably close match, giving confidence to the calculation method. Some discrepancy is to be expected, since the values derived from the manufacturer's payload-range diagram assume nominal performance of the aircraft.

For the A320, the average range factor from flight data is about 15% lower than that derived from the aircraft specification. Further investigation of the flight data revealed that the A320 aircraft were routinely operated on short-range missions with highly variable payloads. As shown by Eq. (3), H depends only on the engine efficiency and the aircraft lift-to-drag ratio during cruise, so short-range flights with low payload do not lead directly to a lower range factor. However, if we consider the aircraft lift coefficient at start-of-cruise, this can be written as

$$C_L = \frac{W_{\mathrm{TOC}}}{\frac{1}{2}\gamma p_{\mathrm{cr}} M_{\mathrm{cr}}^2 A_w} \tag{9}$$

Figure 3 shows a plot of range factor against cruise lift coefficient, both extracted directly from the FDR data for the A320. Also shown is an estimate of the aircraft design point according to the airframe specifications.[§] The plot suggests that the majority of flights in the sample were operated at nonoptimal reduced lift coefficient. This is expected to be a result of ATC and operational restrictions, which prevent the aircraft from flying at a higher altitude or a significantly lower Mach number.

IV. Range-Equation Adjustments

A. Wind Effect

As mentioned before, Rivas et al. [9] concluded in their study that maximum range is strongly affected by wind. This is to be expected, since an aircraft flying against a constant head wind would travel a

[§]See www.airbus.com/aircraftfamilies/passengeraircraft/a320family/a320/specifications [retrieved 6 May 2011].

much greater air distance than a flight in still air, yet still cover the same ground track.

To isolate the effect of the wind, the air distance of each flight was extracted from the flight data. This was done using each point in the flight trajectory by taking the product of the time between recorded events and the averaged airspeed. The following equation illustrates this as

$$\delta s_{\text{air}} = \left(\frac{V_i + V_{i+1}}{2}\right)(t_{i+1} - t_i) \tag{10}$$

where V_i is the airspeed at a given event, t_i is the time the event occurred, and δs_{air} is the air distance between consecutive events. Note that although the time interval varied between 5 and 40 s, depending on the stage of flight, this approach is still robust. As for the latter (larger) time interval, the aircraft would be in the cruise phase, and therefore the velocity is almost constant.

The air distance of the entire cruise period was then determined from these data and used to calculate a new range factor H_{air}. Figure 4 shows distributions for this range factor and for the range factor based on measured ground-track distance. It clearly shows that there is reduced variation using the air-distance-derived range factor, indicating that the aircraft performance is more consistent once the wind is accounted for. This makes sense, since the range factor is a measure of the performance of the aircraft as it moves relative to the air. It is also worth noting that the variation of H_{air} resembles a Poisson distribution, in which the maximum value is close to the mean and the performance smoothly degrades to lower values. This observation could be useful for detailed statistical modeling of aircraft fuel burn.

For a simple model, the fuel burn as a function of ground-track distance is preferred, since it is ground-track distance that is readily available for a flight, either from flight-planning information or regular surveillance data. The average ground speed of the aircraft is the average airspeed minus any headwind:

$$V_{\text{gr}} = V_{\text{air}} - V_{\text{HW}} \tag{11}$$

The air distance traveled can then be expressed in terms of the ground-track distance as follows:

$$s_{\text{air}} = s_{\text{gr}}\frac{V_{\text{air}}}{V_{\text{gr}}} = s_{\text{gr}}\left(\frac{V_{\text{air}}}{V_{\text{air}} - V_{\text{HW}}}\right) \tag{12}$$

This can be written as

$$\frac{s_{\text{air}}}{s_{\text{gr}}} = \left(1 - \frac{V_{\text{HW}}}{V_{\text{air}}}\right)^{-1} \tag{13}$$

Using the flight data, the parameters $s_{\text{air}}/s_{\text{gr}}$ and $V_{\text{HW}}/V_{\text{air}}$ were determined for the cruise phases of all the flights available. The results are plotted in Fig. 5 for the B777 aircraft and compared with Eq. (13), which is close to a best fit. A similar level of agreement was found for the flight data from all the aircraft types.

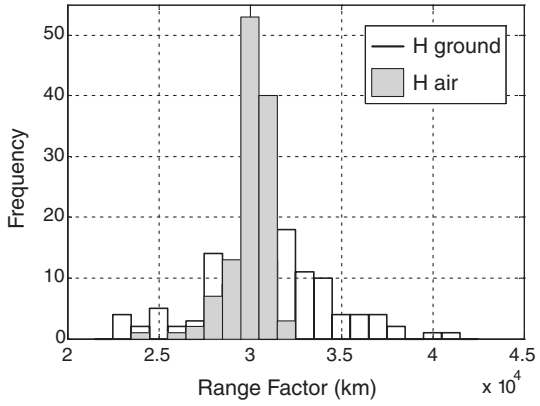

Fig. 4 Distribution of range factors derived using air and ground distances for B777 data.

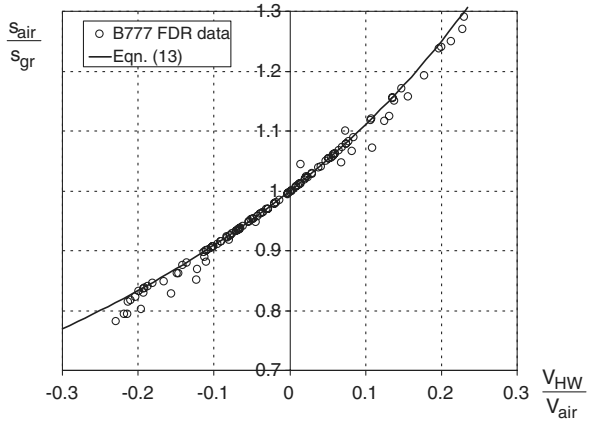

Fig. 5 Relationship between average headwind and air distance for B777 aircraft using FDR data.

The above analysis suggests that for an improved estimation of fuel burn, the air distance should be used and that this can be estimated from the ground-track distance using Eq. (13). The air distance is incorporated into the basic fuel-burn model, Eq. (7), as follows:

$$\begin{aligned} W_{\text{fuel}} &= W_{\text{TO}}\left(1 - \exp\left\{\frac{-s_{\text{air}}}{H_{\text{cr}}}\right\}\right) \\ &= W_{\text{TO}}\left(1 - \exp\left\{\frac{-s_{\text{gr}}}{H_{\text{cr}}(1 - V_{\text{HW}}/[M_{\text{cr}}\sqrt{\gamma R T_{\text{cr}}}])}\right\}\right) \end{aligned} \tag{14}$$

where M_{cr} is the cruise Mach number and T_{cr} is the ambient temperature at the cruise altitude, which can be calculated using the International Standard Atmosphere. The cruise range factor H_{cr} is the range factor corresponding to the cruise conditions of the particular flight of interest. It can be determined by scaling the nominal (or design) range factor using

$$H_{\text{cr}} = H_{\text{nom}}\left(\frac{V_{\text{air}}}{V_{\text{nom}}}\right) = H_{\text{nom}}\left(\frac{M_{\text{cr}}\sqrt{T_{\text{cr}}}}{M_{\text{nom}}\sqrt{T_{\text{nom}}}}\right) \tag{15}$$

where the nominal range factor H_{nom} is the value derived from manufacturers' data [10], as shown in Fig. 2 for several aircraft types. The nominal cruise conditions in Eq. (15) should also be those given in the aircraft specifications. For example, Boeing specifies that the design altitude and speed for cruise of the B777-300 are 35,000 ft and $M = 0.84$.¶ It should be noted that scaling of the range factor according to Eq. (15) does not account for any changes in engine performance or aircraft lift-to-drag ratio that may arise as a result of a different cruise condition. As demonstrated by Fig. 3, aircraft that are operated far from their nominal cruise condition will have poor performance, leading to reduced range factor. Therefore, the cruise range factor derived using Eq. (15) is only expected to be accurate for cruise conditions fairly close to nominal, and in other cases, H_{cr} should be recalculated using aircraft performance data.

B. Climb Fuel Burn

In addition to providing a means to calculate the total mission fuel, Eq. (14) can be used to predict the cumulative fuel burn at each point along a flight trajectory. This is shown in Fig. 6 and compared with the FDR data for a typical B777 flight. The figure includes the fuel burn predicted by the standard range equation with no adjustment for wind, Eq. (7), as well as the fuel burn given by Eq. (14).

For the particular flight shown in Fig. 6, the average headwind during the cruise was 38 ms^{-1} and the overall profile was representative of a typical long-haul B777 flight. This flight was chosen to illustrate the difference of using the air distance in the fuel-burn prediction, which has a more prominent effect at higher wind speeds. Equation (14) gives a better prediction for the fuel-burn rate during

¶See http://www.boeing.com/commercial/777family/pf/pf_300product.html [retrieved 6 May 2011].

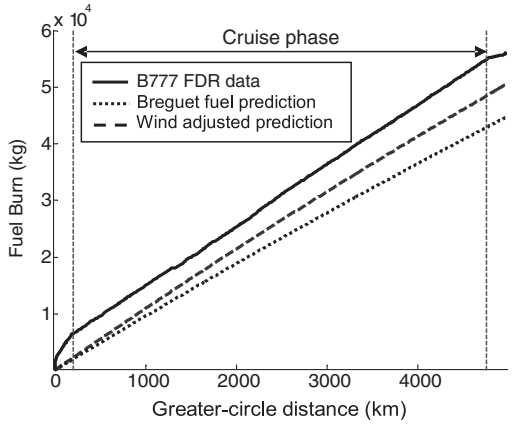

Fig. 6 Actual and predicted fuel burn for a single flight from B777 FDR data.

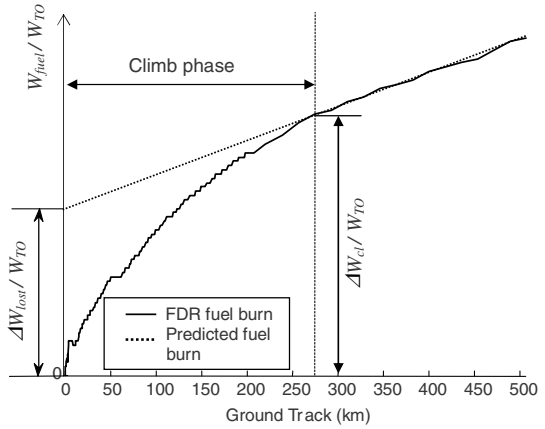

Fig. 7 Aircraft fuel burn during the climb phase.

cruise, seen graphically through a closer match to the actual fuel-burn gradient.

What is also evident in Fig. 6 is that there is still a significant discrepancy between the actual and predicted fuel burn: the actual fuel burn is offset from the model by a fixed amount from the start-of-cruise. The range-equation models the fuel burn by assuming a hypothetical flight at cruise conditions over the total range. However, during the takeoff and climb phase it is seen that the aircraft burns fuel at a greater rate, which can be attributed to two factors. First, the aircraft is performing at a lower efficiency during this stage, as it operates away from the most efficient configuration and operating point. Second, extra fuel must be consumed to accelerate the aircraft to cruising speed and to gain altitude. This extra fuel was termed by Torenbeek [8] as the "lost fuel." The formal definition that is proposed by Torenbeek is that this fuel represents "the difference in fuel that is actually burnt during the climb and the fuel consumed during a cruising flight over the same distance." In this paper, the same definition will be used. However, it should be remembered that this fuel is not strictly lost, as some of the resulting gain in potential and kinetic energy of the aircraft is useful and could be recovered during the descent phase, as is shown later.

Figure 7 is a diagram that illustrates the lost fuel and the fuel burn to top-of-climb, with FDR data taken from a typical B777 flight.

The lost-fuel fraction can be determined from the flight data using

$$\frac{\Delta W_{\text{lost}}}{W_{\text{TO}}} = \frac{\Delta W_{\text{cl}}}{W_{\text{TO}}} - \left(1 - \exp\left\{\frac{-s_{\text{cl}}}{H_{\text{cr}}}\right\}\right) \tag{16}$$

where s_{cl} is the air distance from takeoff to top-of-climb and ΔW_{cl} is the total weight of burned fuel covering this distance. Table 2 shows the mean and range of the lost-fuel parameter, $\Delta W_{\text{lost}}/W_{\text{TO}}$, extracted from the FDR data for each aircraft type. The ranges of values shown were determined from the mean value ± 2 standard deviations.

Table 2 Lost-fuel values derived from the FDR data

Aircraft	Mean lost fuel from FDR $\Delta W_{\text{lost}}/W_{\text{TO}}$, %	Range of values, %
A320	1.60	1.17 → 2.04
A330	1.52	1.17 → 1.87
A340	1.55	1.21 → 1.89
B757	1.61	1.32 → 1.89
B767	1.53	1.35 → 1.71
B777	1.31	1.09 → 1.52

Note that across all aircraft types, the average lost fuel from the flight data is 1.52% of the takeoff weight, and the range of values shows that this is fairly consistent between flights and across different aircraft types.

Previous work, such as by Torenbeek [8] and Roskam [16], included methods for determining the additional fuel burn during takeoff and climb. In 1985, Roskam [16] suggested that a jet-engine-powered transport aircraft will typically have $\Delta W_{\text{cl}}/W_{\text{TO}} \sim 0.025$, or 2.5%. Taking account of the ground distance traveled during climb, which is typically about 250 km, the expected lost-fuel fraction, $\Delta W_{\text{lost}}/W_{\text{TO}}$, would be approximately $2.5\% - 1\% = 1.5\%$, which agrees well with the FDR results above. However, Roskam [16] also provided a plot that suggests that for high-subsonic-Mach-number aircraft, such as those considered here, the fuel burn required during climb should be significantly greater.

Torenbeek [8] determined the lost fuel based on conservation-of-energy arguments, and this approach was applied in [17] to kerosene-powered jet aircraft flying at 35,000 ft and Mach 0.85. The lost-fuel fraction calculated in this case was 2.2%, which is significantly greater than the average values in Table 2. However, it is worth noting that this 2.2% of lost fuel also includes some fuel for en route maneuvering. Poll [12] suggested a typical value of 2.5% of takeoff weight to account for all the additional fuel burn, relative to cruise, during a flight. It is also acknowledged here that the overall fuel-burn performance of an aircraft is very sensitive to this parameter.

Following an approach similar to Torenbeek [8], a method to determine $\Delta W_{\text{lost}}/W_{\text{TO}}$ using limited flight information is explored in Appendix A. The analysis in Appendix A suggests that the spread of values in Table 2 could be due to variations in the length of the climb distance and cruise altitude. The analysis also shows that the average fuel efficiency during climb for the aircraft types analyzed is about 80% of that at cruise.

A fuel-burn equation that incorporates the lost fuel takes the following form:

$$W_{\text{fuel}} = W_{\text{TO}}\left(1 - \exp\left\{\frac{-s_{\text{gr}}}{H_{\text{cr}}(1 - V_{\text{HW}}/[M_{\text{cr}}\sqrt{\gamma RT_{\text{cr}}}])}\right\} + \frac{\Delta W_{\text{lost}}}{W_{\text{TO}}}\right) \tag{17}$$

C. Descent Phase

The model represented by Eq. (17) assumes that during descent, approach, and landing, the aircraft consumes an amount of fuel equal to that consumed by a cruise over the same great-circle distance. This was the assumption used by Torenbeek [8] in his reconsidered range equation, which he acknowledged was a conservative approximation. As indicated in Fig. 6 by the lower slope of the recorded fuel burn after the cruise phase, the fuel-burn rate during descent is different from that during cruise, and this should be taken into account in an improved model.

During descent the engines will be throttled back, resulting in a lower fuel-burn rate for the majority of this phase. However, this is not the complete story, as there are other operational factors that must be considered. Reynolds [10] identified total ground-track extension as one measure of flight inefficiency. For the arrival phase, this track extension manifests itself in several ways. First, the aircraft must align itself with the runway heading at the appropriate distance to

intercept the glide slope. It is then subject to ATC once within a certain range of the airport and may undergo additional vectoring and holding to account for high traffic levels.

If the distance traveled for the descent phase is further than the predicted great-circle distance, the corresponding fuel burn will be increased. In addition, the nondimensional drag of the airframe will generally be greater during descent than during cruise. However, as mentioned above, the engines are burning fuel at a lower rate during this period. Thus, there are competing effects that determine the overall fuel burn for this phase, and it is difficult to estimate the balance of these without knowing the idling engine fuel-burn rate, the change in airframe aerodynamic performance, and the expected track extension. The latter of these factors varies considerably from flight to flight and region of operation, hence the simple assumption that Torenbeek [8] adopted. In this study, the FDR data were analyzed to calculate the recovered fuel. This is defined as the reduction in fuel burn during descent relative to that which would be burned at cruise over the same great-circle distance. The equation used to calculate this is as follows:

$$\frac{\Delta W_{\text{rec}}}{W_{\text{TO}}} = \frac{W_{\text{EOC}}}{W_{\text{TO}}}\left(1 - \exp\left\{\frac{-s_{\text{gc},d}}{H_{\text{cr}}(1 - V_{\text{HW}}/[M_{\text{cr}}\sqrt{\gamma R T_{\text{cr}}}])}\right\}\right) - \frac{\Delta W_d}{W_{\text{TO}}} \tag{18}$$

where $s_{\text{gc},d}$ is the great-circle distance from end-of-cruise to touchdown, and ΔW_d is the weight of fuel burned during descent. The mean recovered-fuel fraction for each aircraft type is shown in Table 3. Also shown is the range of values, again determined using the mean plus and minus 2 standard deviations. For the A320, A340, and B757, the assumption that Torenbeek [8] used, of zero recovered fuel, appears to be reasonably valid. For the A330, B767, and B777, there is a substantial, positive recovered-fuel fraction (around 0.2% of takeoff weight). This may be a result of these aircraft being used on longer-range flights for which a more optimal descent trajectory is possible. However, it is more interesting to consider the range of values and, in particular, to note that the variation between flights is very high and greater than the lost-fuel variation during climb (Table 2). There are flights for all aircraft types for which the recovered-fuel fraction is 0.4% of takeoff weight or greater. This suggests that there is scope for reducing fuel burn by ensuring that more flights follow consistent low-fuel-burn descent procedures.

D. Final Model

The final model for total fuel burn that incorporates all the modifications described above can be written as

$$W_{\text{fuel}} = W_{\text{TO}}\left(1 - \exp\left\{\frac{-s_{\text{gr}}}{H_{\text{cr}}(1 - V_{\text{HW}}/[M_{\text{cr}}\sqrt{\gamma R T_{\text{cr}}}])}\right\} + \frac{\Delta W_{\text{lost}}}{W_{\text{TO}}} - \frac{\Delta W_{\text{rec}}}{W_{\text{TO}}}\right) \tag{19}$$

Note that H_{cr} is the aircraft range factor corresponding to the cruise altitude and Mach number of the flight. Equation (19) requires values for the lost and recovered fuel, which could be derived empirically from fleet average values. Alternatively, the procedure in Appendix A can be followed to estimate the lost fuel during climb. In the following section, the model above is validated against a further set of flight data, using $\Delta W_{\text{lost}}/W_{\text{TO}} = 0.0152$ and $\Delta W_{\text{rec}}/W_{\text{TO}} = 0.001$, which are the mean values from Tables 2 and 3 across all the aircraft types.

Note that the ground-track distance s_{gr} in Eq. (19) is the total ground-track distance of the flight, excluding any ground-track extension necessary during descent. This total distance could be approximated as the great-circle distance s_{gc} if details of the flight path are not known. Otherwise, data from flight-planning programs or conventional surveillance sources could be used. The headwind speed V_{HW} is the mean headwind component during the flight. This could be estimated from averaged forecast or historical weather data for the flight trajectory.

Table 3 Recovered fuel during descent derived from the FDR data

Aircraft	Mean recovered fuel $\Delta W_{\text{rec}}/W_{\text{TO}}$, %	Range of values, %
A320	−0.06	−0.70 → 0.58
A330	0.27	−0.06 → 0.60
A340	0.07	−0.56 → 0.70
B757	−0.08	−0.56 → 0.40
B767	0.27	−0.09 → 0.64
B777	0.15	−0.09 → 0.40

V. Model Validation

To test the fuel-burn modeling, a new set of FDR data was used, which contained a reduced number of recorded flight parameters for each flight but included a much larger number of flights (see Table 4). This new set of data is referred to as reduced FDR data.

The model was assessed by finding the difference between the actual total fuel burn in the FDR data and the predicted total fuel burn. The following error parameter allows the accuracy of each model to be compared across the flights for each aircraft, irrespective of flight distance:

$$\text{error} = \frac{\text{actual fuel burn} - \text{model fuel burn}}{\text{actual fuel burn}} \times 100\% \tag{20}$$

Each stage of the model development is now presented successively to illustrate the effect of the modifications individually. To begin with, the flight information was entered into the original Bréguet range equation (7), using the nominal aircraft range factor given in [10]. The results for the A330 are shown in Fig. 8.

Figure 8 shows that, in general, the range equation underestimates the amount of fuel needed for a flight. This is consistent with expectation, as it takes no account of the lost fuel or the wind speed. In cases in which the error is low, this is expected to be due to high tailwinds, compensating for the extra fuel needed for climb.

The effect of introducing the empirically derived lost- and recovered-fuel factors (0.0152 and 0.001, respectively) can be seen in Fig. 9. The probability density function has not increased, but the distribution has been shifted left, so that the mean fuel error sits almost on zero.

The shape of the distribution in Fig. 9 is intriguing and can be best explained by plotting the headwind distribution (Fig. 10). The headwind distribution appears to be the sum of two normal distributions, around −25 and +20 m/s, respectively. This suggests that the A330 has been flown on routes with strong prevailing winds, i.e., outbound there is a headwind, inbound there is a tailwind.

Equation (19), using the empirically derived lost- and recovered-fuel factors, as well as the estimated total air distance gives the distribution shown in Fig. 11. The error distribution for this shows a normal distribution with the mean centered just above zero and a range of −10 to +15% error. This is a large improvement when compared with the original Bréguet range equation and shows quite convincingly that the adaptations to the range equation are appropriate.

Table 4 Aircraft used in model validation with reduced specification FDR data

Aircraft	Abbreviation	Number of flights
A320-214	A320	1794
A330-243	A330	1433
A340-300	A340	1293
B777-300	B777	966

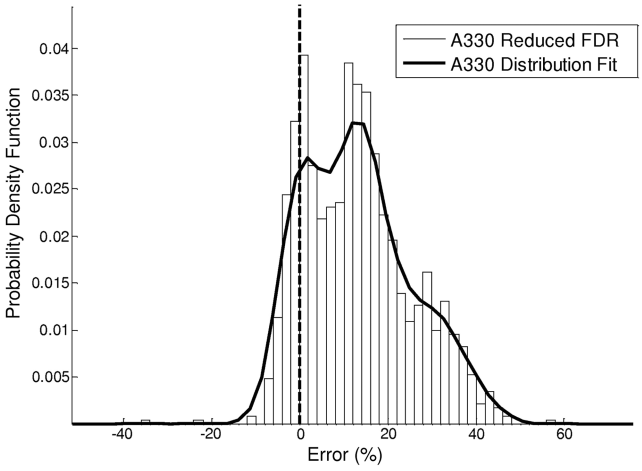

Fig. 8 Error distribution for the classical range equation applied to reduced A330 FDR data [Eq. (7)].

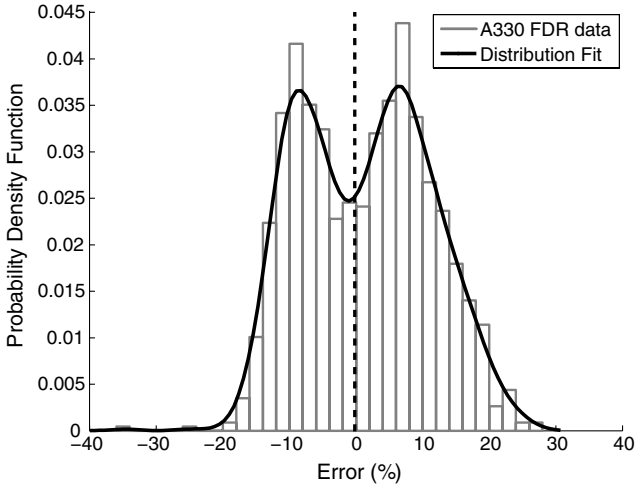

Fig. 9 Error distribution for fuel-burn prediction using a fuel offset, but no account of wind, applied to the reduced A330 FDR data.

The mean values of error and standard deviation of the error for the reduced specification flight data are detailed in Table 5 for both the final model and the simple Bréguet range equation. In all cases, both the mean error and the standard deviation have decreased significantly.

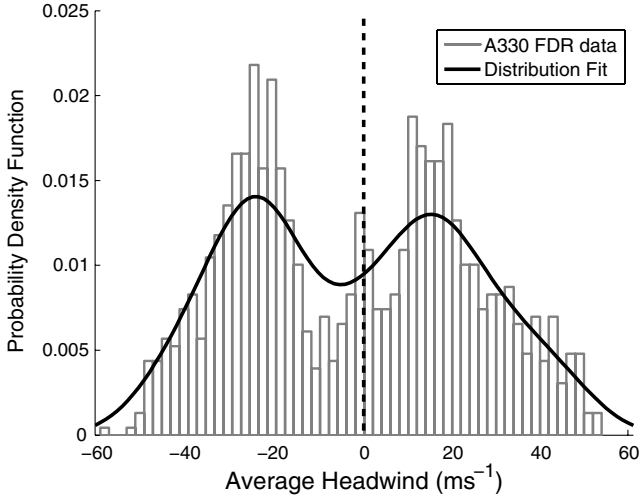

Fig. 10 Distribution of average headwind component for each flight in the reduced A330 FDR data.

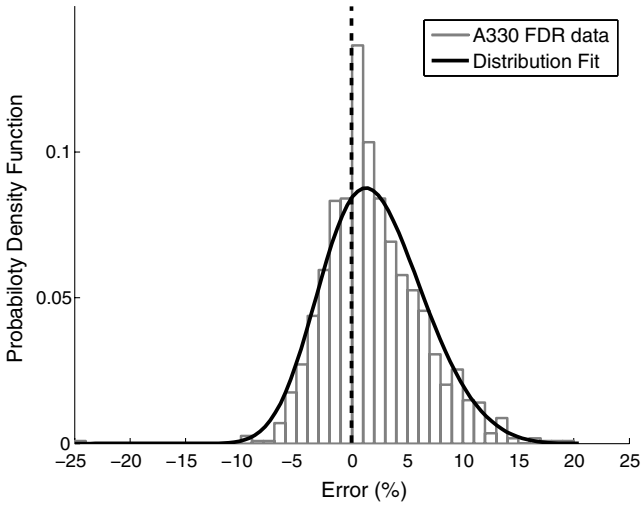

Fig. 11 Error distribution for final fuel-burn prediction with an average offset and adjusted for wind applied to the reduced A330 FDR data [Eq. (19)].

VI. Conclusions

An investigation of several aircraft types has shown that, on average, the cruise performance achieved in practice is close to that expected from the aircraft specification. However, it has also been found that aircraft can suffer a significant performance penalty in service if they are operated at a lift coefficient lower than a nominal cruise value.

Analysis of flight data has shown that for accurate fuel-burn prediction, the total air distance should be used in the range equation. This can be estimated by scaling the ground-track distance to account for the average headwind. The range factor used to model the aircraft performance in the range equation should also be appropriate to the aircraft cruise condition for the particular flight of interest.

The extra fuel burned during the takeoff and climb of a modern passenger aircraft has been calculated from measured data. Across the six aircraft types studied, the average additional fuel was found to be 1.52% of the takeoff weight, which is the same as, or slightly lower than, the values assumed in previous studies. This additional fuel is used in increasing the aircraft kinetic and potential energy as well as overcoming additional drag during the climb phase.

The fuel used during descent of a passenger aircraft can be considerably less than that which would be required to cruise over the same great-circle distance. However, the sample of flight data studied suggests that there is a large variation in the descent fuel burn due to variation in the operation of the aircraft and the trajectory followed up to touchdown. The analysis in this paper suggests that there is the potential to recover a substantial amount of fuel burn through more consistent approach procedures.

Finally, it has been shown that through several simple adjustments, a more accurate model for fuel burn than the simple Bréguet range equation can be derived. For the three long-range aircraft in question, the A330, A340, and B777, the maximum mean error was less than 2% when the new model was tested on a large sample of flight data. This is a dramatic improvement on the error that was given using the simple range equation. The standard deviation of the error for each

Table 5 Comparison of the accuracy of the Bréguet range equation and new fuel prediction model

Aircraft	Bréguet range equation (7)		Final model (19)	
	Mean error ε, %	Standard deviation σ, %	Mean error ε, %	Standard deviation σ, %
A320	35.82	9.56	10.08	5.93
A330	13.25	13.33	1.95	4.32
A340	5.66	20.11	−1.15	3.64
B777	8.86	8.63	0.37	4.14

aircraft has also been significantly reduced. That said, the final model does have its limitations, and its derivation is based on the assumption that it is applied to typical flight operations of modern turbofan-powered passenger aircraft.

Appendix A: Estimating the Lost Fuel During Climb

The fuel burned during climb is used to increase the aircraft kinetic energy, to raise the aircraft potential energy, and to do work against the airframe drag. Assuming that during climb, the engine is operating at a constant overall efficiency η_{cl} and the aircraft is operating at a reduced-but-constant range factor H_{cl}, the fuel burn during climb can be written as

$$\Delta W_{cl} = \frac{\Delta PE + \Delta KE}{\eta_{cl} LCV} + W_{TO}\left(1 - \exp\left\{\frac{-s_{cl}}{H_{cl}}\right\}\right) \tag{A1}$$

The aircraft range factor and the engine overall efficiency are related via Eq. (3). Using this and the approximation that the aircraft weight is constant during climb, Eq. (A1) can be rewritten as

$$\frac{\Delta W_{cl}}{W_{TO}} \cong [(h + V^2/2g)(L/D) + s_{cl}]/H_{cl} \tag{A2}$$

The ratio of the range factor during climb to the adjusted range factor at cruise is given by

$$k_{cl} = \frac{H_{cl}}{H_{cr}} \tag{A3}$$

The value of k_{cl} was determined from the FDR data for each flight. For this, Eq. (A2) was used to derive the climb range factor, assuming an aircraft lift-to-drag ratio equal to the value at cruise. An average range-factor ratio was then determined for each aircraft type, which is included in Table A1. Using this average ratio of range factors, the lost fuel for any flight can then be estimated using

$$\frac{\Delta W_{lost}}{W_{TO}} \cong [(h + V^2/2g)(L/D) + s_{cl}]/(\bar{k}_{cl} H_{cr}) - s_{cl}/H_{cr} \tag{A4}$$

The average lost fuel calculated using Eq. (A4) is included in Table A1 for each of the aircraft types. The values agree reasonably well with the actual lost-fuel values derived from FDR data in Table 2.

A disadvantage of the above approach is that is requires information about the air distance of the climb phase, s_{cl}. Using the flight data, the average aircraft climb distance was found to be around 250 km for a range of flights and aircraft types. However, the FDR data also show that, in practice, there is a large variation in the climb distance between individual flights, which is probably a result of variations in the operating procedures and ATC restrictions. This means that there could be significant error in Eq. (A4) if this is applied to a single flight in which the climb distance is not known in advance.

Note that the ratio of range factors k_{cl} is between 0.76 and 0.84 for all the aircraft types. Hence, a reasonable estimate of k_{cl} for all aircraft would be 0.8. This suggests that during typical climb procedures, aircraft have, on average, 80% of the fuel efficiency of that during cruise, which is a believable value. The reduced efficiency will be due mainly to the reduced flight speed, which reduces the engine propulsive efficiency, and partly due to reduced lift-to-drag ratio, particularly during the early stages of climb, when the configuration of the airframe is not clean.

Table A1 Calculation of lost fuel

Aircraft	Average range-factor ratio $\bar{k}_{cl}$	Calculated lost fuel $\Delta W_{lost}/W_{TO}$, %
A320	0.838	1.65
A330	0.779	1.51
A340	0.759	1.61
B757	0.815	1.64
B767	0.772	1.51
B777	0.779	1.35

Acknowledgments

The authors would like to thank Swiss International Air Lines, Ltd., for provision of the flight data presented. They would like to acknowledge the support for this work from the Cambridge University Engineering Department, the Aviation Integrated Modelling (AIM) project, and the Sir Arthur Marshall Institute for Aeronautics. The authors would also like to thank Nick Cumpsty, Tom Hynes, and Will Graham for very helpful technical discussions and feedback during the preparation of this paper.

References

[1] Cavcar, M., "Bréguet Range Equation?," *Journal of Aircraft*, Vol. 43, No. 5, 2006, pp. 1542–1544. doi:10.2514/1.17696

[2] Bréguet, L., "Calcul du Poids de Combustible Consummé par un Avion en vol Ascendant," *Comptes Rendus de l'Academie des Sciences*, Vol. 177, 1923, pp. 870–872.

[3] Page, R. K., "Performance Calculation for Jet Propelled Aircraft," *Journal of the Royal Aeronautical Society*, Vol. 55, 1947, pp. 440–450.

[4] Edwards, A. D., "Performance Estimation of Civil Jet Aircraft," *Aircraft Engineering*, Vol. 22, No. 254, 1950, pp. 94–99.

[5] Jonas, J., "Jet Airplane Range Considerations," *Journal of the Aeronautical Sciences*, Vol. 14, 1947, pp. 124–128.

[6] Perkins, C. D., and Hage, R. E., *Airplane Performance, Stability and Control*, Wiley, New York, 1949, pp. 183–194.

[7] Peckham, D. H., "Range Performance in Cruising Flight," Royal Aircraft Establishment, TR 73164, 1974.

[8] Torenbeek, E., "Cruise Performance and Range Predictions Reconsidered," *Progress in Aerospace Sciences*, Vol. 33, Nos. 5–6, 1997, pp. 285–321. doi:10.1016/S0376-0421(96)00007-3

[9] Rivas, D., Lopez-Garcia, O., Esteban, S., and Gallo, E., "An Analysis of Maximum Range Cruise Including Wind Effects," *Journal of Aerospace Science and Technology*, Vol. 14, No. 1, 2010, pp. 38–48. doi:10.1016/j.ast.2009.11.005

[10] Martinez-Val, R., Palacin, J. F., and Pérez, E., "The Evolution of Jet Airliners Explained Through the Range Equation," *Proceedings of the Institution of Mechanical Engineers, Part G (Journal of Aerospace Engineering)*, Vol. 222, No. 6, 2008, pp. 915–919. doi:10.1243/09544100JAERO338

[11] Cavcar, M., and Cavcar, A., "Comparison of Generalized Approximate Cruise Range Solutions for Turbojet/Fan Aircraft," *Journal of Aircraft*, Vol. 40, No. 5, 2003, pp. 891–895. doi:10.2514/2.6879

[12] Poll, D. I. A., "The Optimum Aeroplane and Beyond," *The Aeronautical Journal*, Vol. 113, No. 1141, 2009, pp. 151–164.

[13] Reynolds, T. G., "Development of Flight Inefficiency Metrics for Environmental Performance Assessment of ATM," *Air Traffic Management Research and Development Seminar*, NAPA, June–July 2009.

[14] Vera-Morales, M., and Hall, C. A., "Modeling Performance and Emissions from Aircraft for the Aviation Integrated Modelling Project," *Journal of Aircraft*, Vol. 47, No. 3, 2010, pp. 812–819. doi:10.2514/1.44020

[15] *Admiralty Manual of Navigation*, 6th ed.,Stationary Office, London, 1997.

[16] Roskam, J., *Airplane Design, Part I: Preliminary Sizing of Airplanes*, Roskam Aviation, Ottawa, KS, 1985.

[17] Green, J. E., "Greener by Design—The Technology Challenge," *The Aeronautical Journal*, Vol. 106, No. 1056, 2002, pp. 57–113.